eISSN: 2721-5717; pISSN: 2747-2124 https://journal.unhas.ac.id/index.php/zonalaut

ZONA LAUT

JOURNAL OF OCEAN SCIENCE AND TECHNOLOGY INNOVATION

Stability Analysis of Floating Platforms for Supporting Renewable Energy-Powered Oil Skimmer Systems

Ahmad Yasim*[1], Muhammad Irsan[2], Andi Widiasari Maruddani[1], Wahyu Syafala Basri[1]
[1]Study Program of Naval Architecture, Bacharuddin Jusuf Habibie Institute of Technology, Parepare, Indonesia
[2]Study Program of Electrical Engineering, Bacharuddin Jusuf Habibie Institute of Technology, Parepare, Indonesia
*ahmadyasim@ith.ac.id

Abstract

Oil spills in marine waters pose serious environmental and economic challenges, requiring effective and sustainable response technologies. Floating oil skimmer systems powered by renewable energy offer a promising solution; however, their operational performance strongly depends on the stability of the supporting floating platform. This study aims to evaluate the stability characteristics of three barge-type floating platform designs intended to support a renewable energy-powered oil skimmer system. Stability analysis was conducted by determining the hydrostatic characteristics, KG, GM, and GZ curves using several loading conditions, including full load, lightship, and ballast conditions. The stability performance of each design was evaluated according to the IMO Intact Stability Code (2008). The results indicate that all three platform designs satisfy the IMO stability criteria under full-load conditions, with Barge 1 demonstrating the best performance, achieving the highest values of GM_0, GZ_{max}, and GZ area. Under lightship conditions, however, all designs failed to satisfy the minimum GZ_{max} angle criteria due to the relatively high KG. Stability improvements were achieved by introducing ballast water, where a minimum ballast level of 75% was required to satisfy the intact stability criteria. Furthermore, the platform could safely operate without ballast once the oil storage tanks reached at least 45% capacity. These findings demonstrate that Barge 1 provides the most favorable stability characteristics and is the most suitable platform configuration for supporting a renewable energy-powered floating oil skimmer system.

Keywords: Floating Platform Oil Skimmer; Stability; Barge; GZ Curve

1. INTRODUCTION

Indonesian waters are characterized by intensive shipping activities and offshore energy resource exploitation, making them highly vulnerable to marine pollution caused by oil spills. Oil spill incidents not only degrade marine ecosystems but also result in significant economic losses, particularly in the fisheries and maritime transportation sectors [1]–[3]. These challenges highlight the need for the development of effective, sustainable, and autonomous technologies for oil spill response in marine environments.

One of the most widely adopted approaches is the use of oil skimmers, which are designed to separate oil from the water surface [4], [5]. Several studies have demonstrated that oil skimmer systems mounted on floating platforms offer considerable flexibility for offshore applications [6]–[9]. Furthermore, integrating these systems with renewable energy sources has emerged as a promising solution for enhancing operational autonomy, particularly in remote areas where access to conventional energy is limited [10]. Nevertheless, the overall performance of such systems is strongly influenced by the design of the floating platform, which serves as the primary support structure for all operational components.

In a previous study [10], a floating oil skimmer system was developed by evaluating several platform configurations, including catamaran and barge types. The results indicated that the barge configuration was more suitable for small-scale applications due to its relatively large buoyancy volume and wider deck area within a single hull structure. In addition, the monohull configuration of a barge offers a simpler structural design and provides greater efficiency in supporting the overall system load. Although catamarans are well known for their superior transverse stability resulting from the wide spacing between their twin hulls [11],

copyright is published under Lisensi Creative Commons Atribusi 4.0 Internasional.

[12], they generally involve higher design and manufacturing complexity and do not necessarily provide significant advantages for relatively small floating platforms. Moreover, when the hull beneath the main deck is intended to function as an oil storage tank, the slender and narrow hulls of a catamaran become less suitable for accommodating sufficient storage capacity.

Despite these advantages, the previously developed barge-type platform still had several limitations, particularly in supporting the optimal integration of renewable energy systems. The relatively limited platform dimensions allowed only solar panels to be installed as the primary energy source, while the integration of wind energy remained impractical. This limitation is primarily attributed to the large vertical dimensions of wind turbines, which may raise the platform's center of gravity and significantly reduce its stability [10].

The combined utilization of solar and wind energy is essential for improving system reliability, considering the dynamic nature of the marine environment and the intermittent availability of renewable energy sources. Therefore, it is necessary to develop a floating platform that is not only capable of supporting the oil skimmer system but also possesses sufficient stability characteristics to accommodate a hybrid renewable energy system.

Based on these considerations, this study was conducted as a continuation of previous research, focusing on the stability analysis of several floating platform design variations. The novelty of this study lies in the development and geometric optimization of a barge-type floating platform designed to maintain adequate stability under the additional vertical loads imposed by wind turbines, combined with the development of a ballast management strategy to support safe platform operation under varying loading conditions. The findings are expected to contribute to the development of more adaptive, reliable, and suitable floating platform designs for renewable energy-powered oil skimmer systems operating in Indonesian waters.

2. METHODS

The stability analysis in this study was conducted to evaluate the ability of the floating platform to maintain equilibrium under external forces, particularly those resulting from the additional loads imposed by the oil skimmer system and renewable energy components. The analysis began with the determination of the hydrostatic characteristics of each platform model, including displacement, buoyancy, and other geometric parameters obtained from design calculations and numerical simulations. The relative positions of the principal stability points, namely the center of gravity (G), center of buoyancy (B), and metacenter (M), determine whether a floating structure exhibits positive stability (M located above G), neutral stability (M coincident with G), or negative stability (M located below G) [13]. When the platform heels, the center of buoyancy shifts due to the change in the submerged volume, generating a restoring moment that tends to return the platform to its equilibrium position. The fundamental principle of this stability mechanism is illustrated in Figure 1.

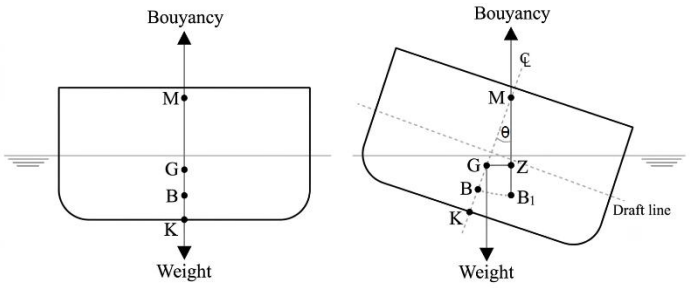


Figure 1. Basic Principle of Ship Stability [14]

The value of KB can be determined using the following equation [15], [16]:

$$KB = \frac{\int_0^{Tp} T\, A_{wp}\ dT}{\nabla} \quad (1)$$

where T is the waterline spacing (m), Tp is the maximum draft (m), A_{wp} is the waterplane area (m²), and ∇ is the displacement volume (m³).

The next step involved determining the position of the center of gravity (G) based on the distribution of the floating platform. The weight contribution and vertical position of each system component, including the main

copyright is published under Lisensi Creative Commons Atribusi 4.0 Internasional.

structure, oil skimmer, batteries, solar panels, and wind turbine, were calculated with respect to the keel as the reference datum. The position of the center of gravity was determined using the static moment approach by dividing the sum of the weight moments by the total system weight, as expressed by the following equation:

$$KG = \frac{\sum W_i z_i}{\sum W_i} \tag{2}$$

where, W_i is the weight of the *i*-th platform component (e.g., lightship, oil skimmer, wind turbine, etc.) (ton), z_i is the vertical distance from the keel to the center of gravity of the *i*-th component (m). Once the heights of the center of buoyancy (KB) and the center of gravity (KG) have been determined, the initial stability of the floating platform can be evaluated by calculating the metacentric height (GM), which is expressed as follows:

$$GM = KB + BM - KG \tag{3}$$

where BM is the metacentric radius (m), which depends on the transverse moment of inertia of the waterplane and the displacement. BM can be calculated using the following equation [17]:

$$BM = \frac{I_T}{\nabla} \tag{4}$$

where I_T is the transverse moment of inertia of the waterplane area (m^4), and ∇ is the displacement volume (m^3).

The calculated GM value was used to evaluate the stability of the floating platform. In general, a larger GM indicates a greater ability of the platform to return to its upright position after heeling. However, an excessively large GM may also result in rapid and abrupt rolling motions (i.e., a *stiff* platform), which should be carefully considered in the design process. To further evaluate the platform stability, the righting arm (GZ) was calculated as a function of the heel angle (θ). The relationship between GZ (m) and the heel angle θ (deg) can be expressed as follows:

$$GZ = GM \cdot sin\,(\theta) \tag{5}$$

The GZ curve is used to describe the platform's ability to generate a righting moment. The righting moment can be determined by multiplying the righting arm (GZ) by the platform displacement, as expressed by the following equation:

$$M_r = \Delta \cdot GZ \tag{6}$$

where M_r is the righting moment (ton.m), and Δ is the platform displacement (ton). The static stability of a floating platform ($\theta \leq 15$ deg) can be evaluated using GZ and M_r, whereas its dynamic stability ($\theta > 15$ deg) is assessed based on the area under the GZ curve [18]. Accordingly, the dynamic stability (ton·m) can be calculated using the following equation:

$$\text{Dynamic Stability} = \int \Delta\, GZ\, \delta\theta \tag{8}$$

Subsequently, the resulting GZ curves were evaluated based on the stability criteria specified in the IMO Intact Stability Code 2008 [19], including the area under the GZ curve over specified heel angle ranges, the maximum GZ value, the heel angle at which the maximum GZ occurs, and the initial GM value [20]. This evaluation was conducted to verify that each platform design satisfies the recommended minimum stability requirements. Through this evaluation process, the principal stability parameters were obtained and subsequently compared among the different platform designs to identify the configuration that provides the most favorable stability performance for supporting a renewable energy-powered oil skimmer system.

copyright is published under Lisensi Creative Commons Atribusi 4.0 Internasional.

3. RESULTS AND DISCUSSION

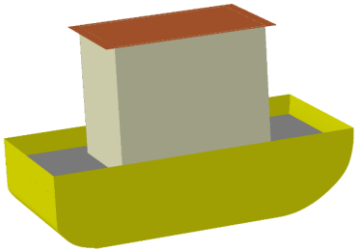
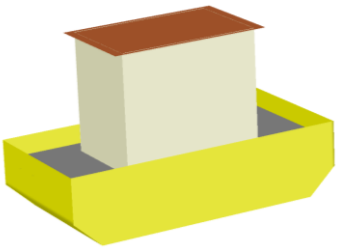
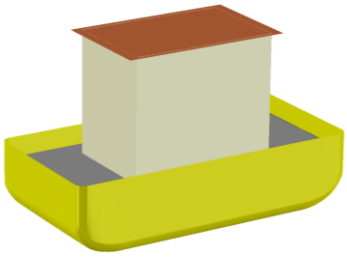
3.1. Design Configuration of the Floating Platform

The principal dimensions of the floating platform were determined using the parent design approach based on the floating platform developed in a previous study. A new platform design was proposed to address the limitations of the previous design, which was considered too small to accommodate the installation of a wind turbine. Therefore, the platform dimensions were increased, and several hull design variations were developed to evaluate their hydrodynamic performance, particularly in terms of stability, which is the primary focus of this study. The principal dimensions and design configurations of the floating platform are presented in Tables 1 and 2, respectively. For clarity, displacement or weight is presented in kilograms (kg) rather than tonnes (ton) throughout the Results and Discussion section, as the floating platforms are relatively small.

Table 1. Principal Dimensions of the Floating Platform

Parameters	Unit	Barge 1	Barge 2	Barge 3
Length Overall (LOA)	m	6	6	6
Length of Waterline (LWL)	m	5.68	6	6
Breadth (B)	m	3	3	3
Depth (H)	m	1.1	1.1	1.1
Draft (T)	m	0.56	0.55	0.55
Diplacement (Δ)	kg	8781.3	9210	9116.8
Deck Area	m^2	17.93	18	18

Table 2. Hull Design Variations of the Floating Platform

Name	Perspective-Bottom View	Perspective-Side View
Barge 1		
Barge 2		
Barge 3		

The hull designs of the floating platform presented in Table 2 were also rendered to provide a more realistic visualization. The rendering process was assisted by artificial intelligence (AI) to depict the platform operating in an oil spill-contaminated marine environment. One of the rendered floating platform designs is presented in Figure 2.

copyright is published under Lisensi Creative Commons Atribusi 4.0 Internasional.

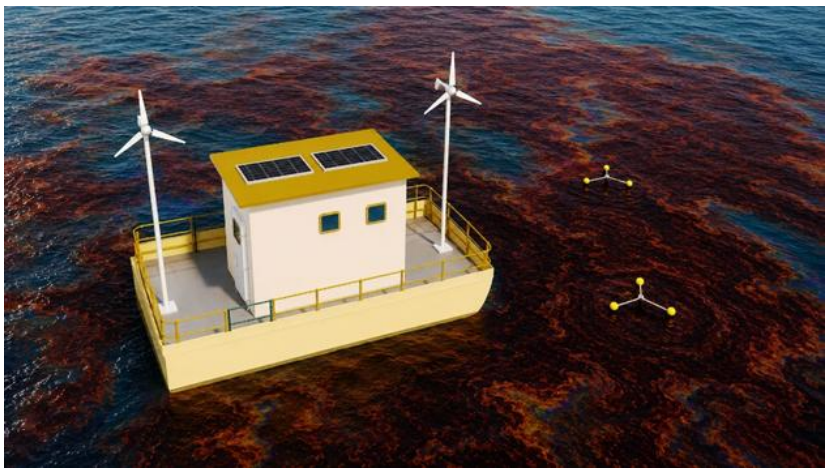


Figure 2. 3D Rendering of the Barge 1 Floating Platform Design

3.2. Loadcase Determination

To analyze the platform stability, appropriate loadcases must first be established to determine the total weight and the KG of the floating platform. One of the most influential load components is the lightship weight. In this study, the lightship weight was determined by developing the platform structure in Maxsurf Structure student version, allowing the lightship weight, LCG, and KG to be calculated with greater accuracy. The floating platform was designed using Aluminum 5083, owing to its excellent corrosion resistance and lightweight properties, which make it one of the most widely used materials for ship hulls and marine structures [21]. One of the structural designs of the floating platform is presented in Figure 3.

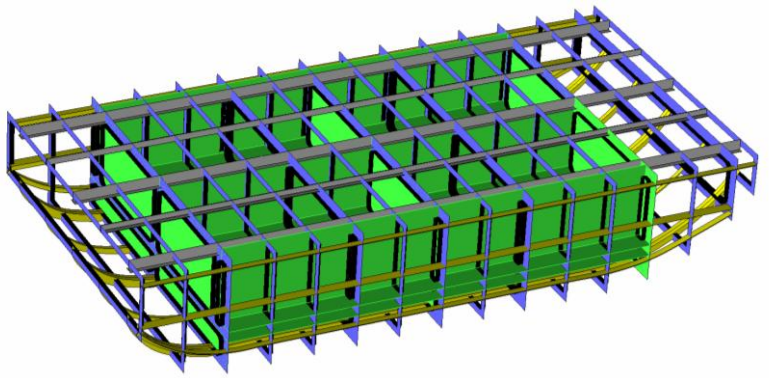


Figure 3. Structural Design of the Barge 1 Floating Platform

The stability analysis in this study was performed under full-load, lightship, and ballast conditions. The total platform weight consists of two main components, namely the lightweight (LWT) and the deadweight (DWT). The LWT includes the weight of the platform structure, wind turbine and solar panels, oil skimmer, piping system, and other auxiliary equipment. Meanwhile, the DWT consists of ballast water, oily water, and recovered oil. The detailed loadcase for the full-load condition is presented in Table 3.

Table 3. Floating Platform Loadcase under Full-Load Condition

Item	Barge 1				Barge 2				Barge 3			
	Qty	Total Weight (Kg)	LCG (m)	VCG (m)	Qty	Total Weight (Kg)	LCG (m)	VCG (m)	Qty	Total Weight (Kg)	LCG (m)	VCG (m)
Lightship	1	2391.3	3.05	1.05	1	2415.8	3.269	1.067	1	2516.7	3.045	1.05
Battery	6	7	3	1.8	6	42	3	1.8	6	42	3	1.8
Oil Skimmer 1	1	130	2.3	1.95	1	130	2.3	1.95	1	130	2.3	1.95
Piping System	1	40	3	1.8	1	40	3	1.8	1	40	3	1.8
Equipment	1	50	3	2	1	50	3	2	1	50	3	2
Oil Skimmer 2	1	130	2.3	1.95	1	130	2.3	1.95	1	130	2.3	1.95

copyright is published under Lisensi Creative Commons Atribusi 4.0 Internasional.

Item	Barge 1				Barge 2				Barge 3			
	Qty	Total Weight (Kg)	LCG (m)	VCG (m)	Qty	Total Weight (Kg)	LCG (m)	VCG (m)	Qty	Total Weight (Kg)	LCG (m)	VCG (m)
Ballast 1P	0%	922.5	2	0.02	0%	0	2.98	0	0%	0	0.91	0
Ballast 1S	0%	922.5	2	0.02	0%	0	2.98	0	0%	0	0.91	0
Ballast 2P	0%	911.4	3.9	0.02	0%	0	5.18	0	0%	0	2.80	0
Ballast 2S	0%	911.4	3.9	0.02	0%	0	5.18	0	0%	0	2.80	0
Oil Tank 1P	95%	1616.7	1.81	0.72	95%	1689.5	1.90	0.73	94%	1519.7	1.79	0.73
Oil Tank 1S	96%	1616.7	1.81	0.72	95%	1689.5	1.90	0.73	94%	1519.7	1.79	0.73
Oil Tank 2P	90%	1616.7	3.81	0.69	85%	1511.6	4.10	0.70	98%	1584.4	3.79	0.74
Oil Tank 2S	90%	1616.7	3.81	0.69	85%	1511.6	4.10	0.70	98%	1584.4	3.79	0.74
Total Loadcase		8781.3	2.86	1.05		9210	3	1.02		9116.8	2.86	0.95

Table 3 presents the loadcases for Barge 1, Barge 2, and Barge 3. Although all three platform designs comprise the same load items, differences in the values of several components arise due to variations in the hull design of each floating platform. The total weight of each load item was determined by multiplying the unit weight by the corresponding quantity installed on the platform. The loadcase also includes environmental loads associated with wind exposure acting on the superstructure and the swept area of the horizontal-axis wind turbine (HAWT), as well as the oil storage tanks and ballast tanks, as illustrated in Figure 4. Both the oil tanks and ballast tanks are fitted with internal bulkheads to reduce the free surface effect, while a cofferdam is provided between the ballast tanks and oil tanks to improve operational safety.

The oil storage capacities of Barge 1, Barge 2, and Barge 3 are 6,691 L, 7,207 L, and 6,989 L, respectively. Each floating platform is equipped with two oil skimmers having the same specifications as those developed in the previous floating oil skimmer study [10]. Each oil skimmer has an oil recovery capacity of 380.16 L/day, resulting in a combined recovery capacity of 760.32 L/day per platform. Based on this recovery capacity, the estimated operating duration before the oil storage tanks reach full capacity is 8.8 days for Barge 1, 9.48 days for Barge 2, and 9.19 days for Barge 3.

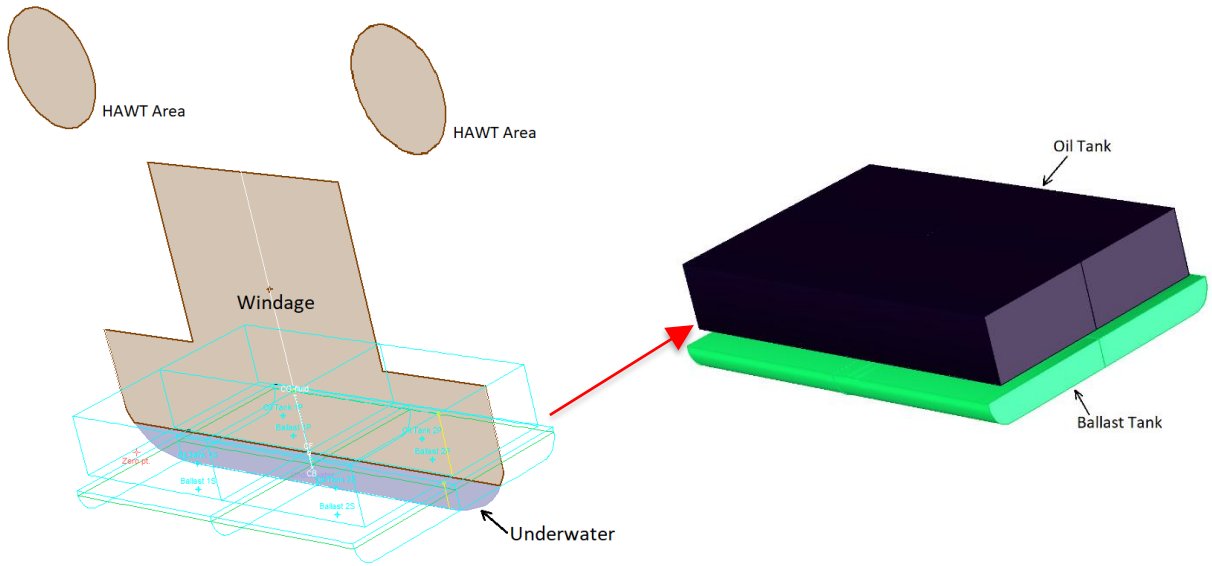


Figure 4. Determination of the Wind-Exposed Area and Inner Tanks

3.3. Stability Analysis under Full-Load Condition

The results of the stability analysis under the full-load condition are presented as GZ curves in Figure 5.

copyright is published under Lisensi Creative Commons Atribusi 4.0 Internasional.

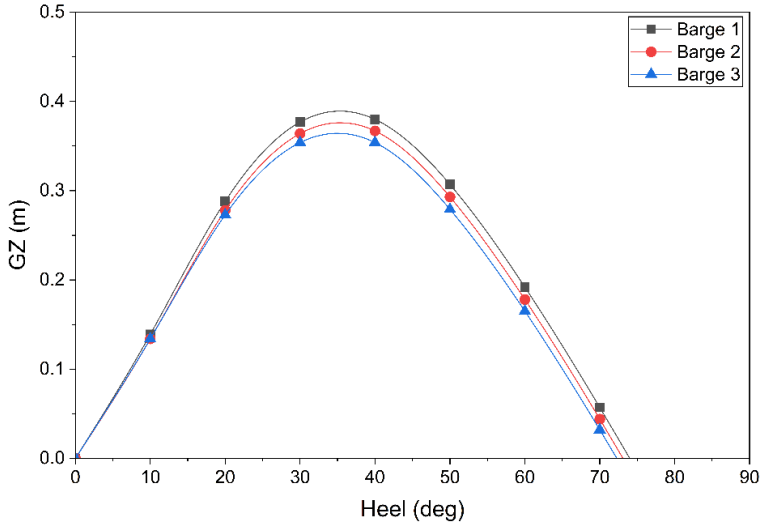


Figure 5. GZ Curves of the Floating Platform under Full-Load Condition

Based on the GZ curves presented in Figure 5, all three floating platform designs exhibit a similar stability trend, with the GZ value increasing as the heel angle increases until reaching a maximum value at the same heel angle of 35.5 deg, after which it gradually decreases and approaches zero at larger heel angles. However, Barge 1 consistently produces higher GZ values than Barge 2, while Barge 3 exhibits the lowest GZ values throughout the entire range of heel angles. This indicates that Barge 1 has a greater ability to generate a righting moment than the other two platform designs. As shown in Figure 5, the GZ curve of Barge 1 remains consistently above those of Barge 2 and Barge 3, resulting in a larger area under the GZ curve. The maximum righting arm (GZ_{max}) of Barge 1 reaches 0.39 m, followed by Barge 2 with 0.38 m and Barge 3 with 0.37 m.

In addition, Barge 1 maintains positive stability up to a heel angle of 74.0 deg, which is slightly higher than Barge 2 (73.0 deg) and Barge 3 (72.4 deg). These results demonstrate that Barge 1 possesses superior stability characteristics, enabling it to maintain equilibrium and generate a greater righting moment under the full-load condition compared with the other platform designs.

Furthermore, the stability performance was evaluated according to the stability criteria specified in the IMO Intact Stability Code (2008). The evaluation results for the full-load condition are summarized in Table 4. As shown in the table, all floating platform designs satisfy the required stability criteria, indicating that each design is considered safe for operation. Nevertheless, Barge 1 demonstrates the best overall stability performance, as evidenced by its larger GZ area and the highest values of GZ_{max} and GM_0 among the three platform configurations.

Table 4. Stability Criteria Evaluation under Full-Load Condition

Stability Criteria (IMO, 2008)		Barge 1		Barge 2		Barge 3	
Parameter	Req.	Actual	Status	Actual	Status	Actual	Status
Area 0^0 to 30^0 (m.deg)	≥ 3.151	6.23	Acc.	6.01	Acc.	5.92	Acc.
Area 0^0 to 40^0 (m.deg)	≥ 5.157	10.09	Acc.	9.73	Acc.	9.53	Acc.
Area 30^0 to 40^0 (m.deg)	≥ 1.719	3.86	Acc.	3.73	Acc.	3.61	Acc.
GZ_{max} at 30^0 or greater (m)	≥ 0.2	0.39	Acc.	0.38	Acc.	0.37	Acc.
Angle of GZ_{max} (deg)	≥ 25	35.5	Acc.	35.50	Acc.	35.50	Acc.
GM_0 (m)	≥ 0.15	0.79	Acc.	0.78	Acc.	0.76	Acc.

3.4. Stability Analysis under Lightship Condition

In addition to the stability analysis under full load conditions, it is equally important to perform stability analysis under the lightship condition. This is since the KG of the floating platform in the light condition is higher compared to the full load condition, resulting from the structural weight being concentrated on the upper main deck. Based on the loadcase determination, the light displacement of Barge 1 is 2783.3 kg with a KG of 1.17 m, Barge 2 is 2807.8 kg with a KG of 1.19 m, and Barge 3 is 2908.7 kg with a KG of 1.17 m. The stability results are presented in the form of GZ curves, as shown in Figure 6. From the figure, it can be observed that

copyright is published under Lisensi Creative Commons Atribusi 4.0 Internasional.

the stability performance of all designs is nearly identical. Furthermore, the trend of the GZ curves is also similar, where the maximum GZ occurs at an angle of heel in the range of 16–17 deg.

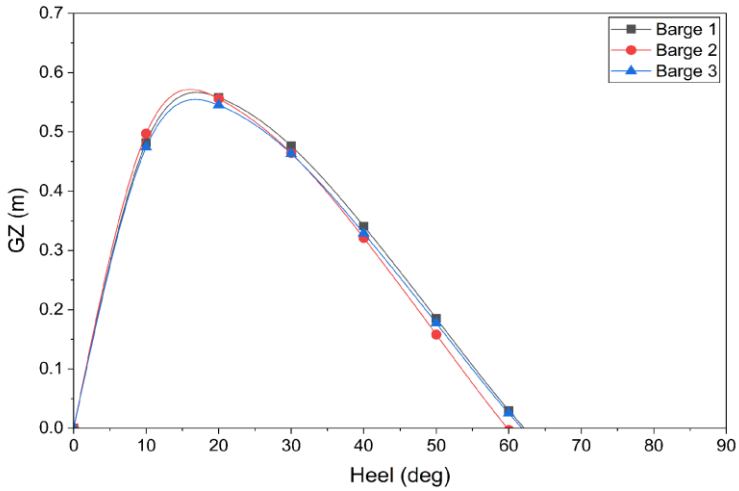


Figure 6. GZ Curve of the Floating Platform under Lightship Condition

The stability evaluation under the lightship condition is presented in Table 5. Based on the evaluation results, it is observed that the intact stability performance of all floating platform designs fails to meet the GZmax angle criterion, which requires that the maximum GZ occurs at a minimum heel angle of 25 deg. Therefore, all three floating platform designs require the addition of ballast at the lower part of the platform to reduce the KG value so that the stability criteria can be satisfied. The ballast used is temporary ballast, in which seawater is filled into the platform; however, when the oil tank reaches a certain level, the ballast water is discharged to maximize the storage capacity of the skimming oil. Accordingly, a further analysis is conducted to determine the minimum ballast requirement to ensure that the floating platform can operate safely under lightship conditions.

Table 5. Evaluation of Stability Criteria under Lightship Condition

Stability Criteria (IMO, 2008)		Barge 1		Barge 2		Barge 3	
Parameter	Req.	Actual	Status	Actual	Status	Actual	Status
Area 0^0 to 30^0 (m.deg)	≥ 3.151	13.36	Acc.	13.46	Acc.	13.07	Acc.
Area 0^0 to 40^0 (m.deg)	≥ 5.157	17.48	Acc.	17.42	Acc.	17.06	Acc.
Area 30^0 to 40^0 (m.deg)	≥ 1.719	4.12	Acc.	3.96	Acc.	3.99	Acc.
GZ_{max} at 30^0 or greater (m)	≥ 0.2	0.48	Acc.	0.46	Acc.	0.46	Acc.
Angle of GZ_{max} (deg)	≥ 25	17.30	Fail	16.40	Fail	16.40	Fail
GM_0 (m)	≥ 0.15	3.07	Acc.	3.18	Acc.	3.14	Acc.

3.5. Initial Ballast Requirement Analysis

The reference parameter used to determine the initial ballast requirement was the GZ_{max} angle criterion (≥ 25 deg), since at ballast levels exceeding 40%, the angle of GZ_{max} criterion was the only intact stability requirement that remained unmet, whereas the other five criteria complied with the requirements of the IMO Intact Stability Code. The results of the minimum ballast requirement analysis are presented in Table 6.

Table 6. Minimum Ballast Requirement

Ballast Level (%)	Barge 1				Barge 2				Barge 3			
	Weight (kg)	KG (m)	Angle of GZ_{max} (deg)	Status	Weight (kg)	KG (m)	Angle of GZ_{max} (deg)	Status	Weight (kg)	KG (m)	Angle of GZ_{max} (deg)	Status
40	4250.3	1.33	20.9	Fail	4426.3	1.35	20	Fail	4481.8	1.34	20	Fail
50	4617.3	1.24	21.8	Fail	4831	1.25	21.8	Fail	4875	1.25	21.8	Fail
60	4984.1	1.16	23.6	Fail	5235.6	1.16	22.7	Fail	5268.3	1.17	22.7	Fail
70	5350.9	1.09	24.5	Fail	5640.2	1.09	24.5	Fail	5661.6	1.10	24.5	Fail

copyright is published under Lisensi Creative Commons Atribusi 4.0 Internasional.

Ballast Level (%)	Barge 1				Barge 2				Barge 3			
	Weight (kg)	KG (m)	Angle of GZ_{max} (deg)	Status	Weight (kg)	KG (m)	Angle of GZ_{max} (deg)	Status	Weight (kg)	KG (m)	Angle of GZ_{max} (deg)	Status
75	5534.5	1.06	25.5	Acc.	5842.5	1.06	25.5	Acc.	5858.2	1.07	25.5	Acc.
80	5717.8	1.04	26.4	Acc.	6044.9	1.04	25.5	Acc.	6054.8	1.04	26.4	Acc.
85	5901.2	1.01	27.3	Acc.	6247.2	1.01	26.4	Acc.	6251.5	1.02	27.3	Acc.

As shown in Table 6, the Barge 1, Barge 2, and Barge 3 designs satisfy the GZ_{max} angle criterion (≥ 25 deg) only when the ballast tanks are filled to at least 75% of their capacity. This behavior is attributed to the sloshing effect, which refers to the free movement of liquid within a partially filled tank during platform motion. The sloshing effect becomes more pronounced as the unfilled volume of the tank increases, allowing the liquid to move more freely. Consequently, sloshing generates a free surface moment (FSM), which reduces the effective metacentric height (GM) and adversely affects the intact stability characteristics. As a result, the required GZ_{max} criterion is achieved only when the ballast tanks are filled to a minimum of 75% capacity.

At a 75% ballast level, the stability performance of the three floating platform designs was further evaluated based on the GZ curves, as shown in Figure 7. The figure confirms that Barge 1 exhibits the best stability performance under the lightship condition with 75% ballast. Furthermore, the GZ curves consistently demonstrate that Barge 1 provides superior stability compared with Barge 2 and Barge 3 across all loading conditions evaluated, including the full load, lightship, and 75% ballast conditions.

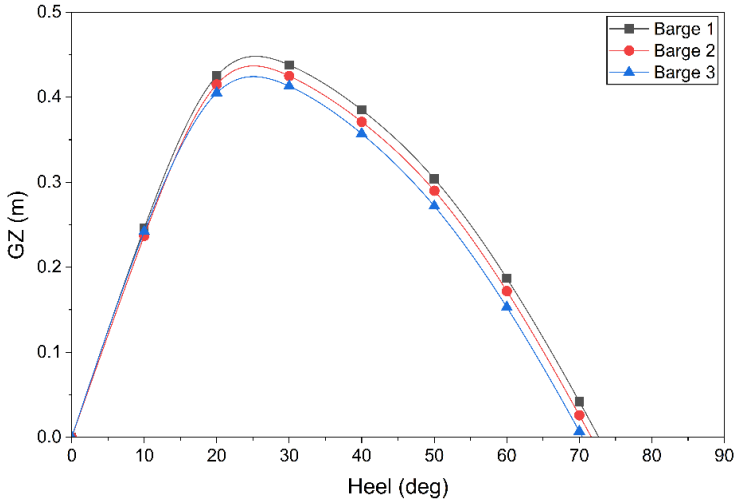


Figure 7. GZ Curves of the Floating Platforms at 75% Ballast Level

3.6. Minimum Oil Tank Filling Level Analysis

Determining the minimum oil tank filling level is necessary to identify the minimum oil volume required to safely discharge the ballast from the floating platform. The analysis procedure is like that used for determining the ballast requirement, in which simulations were performed at various oil tank filling levels. The simulation results indicate that the minimum oil tank filling level required for the platform to operate safely without ballast is 45%. The detailed simulation results are presented in Table 7.

Table 7. Effect of Oil Tank Free Surface Moment on Stability

Oil Tank Level (%)	Barge 1			Barge 2			Barge 3			Angle of GZ_{max} (deg)	Status
	Weight (kg)	FS Corrct (m)	KG (m)	Weight (kg)	FS Corrct (m)	KG (m)	Weight (kg)	FS Corrct (m)	KG (m)		
30	4723.3	0.28	1.17	4941.9	0.29	1.18	5042.8	0.28	1.17	22.7	Fail
35	5046.7	0.26	1.14	5297.5	0.27	1.15	5398.4	0.27	1.13	23.6	Fail
40	5370	0.24	1.11	5653.2	0.25	1.11	5754.1	0.25	1.11	24.5	Fail
45	5693.4	0.23	1.09	6008.9	0.24	1.09	6109.8	0.23	1.08	25.5	Acc.
50	6016.7	0.22	1.07	6364.6	0.23	1.07	6465.5	0.22	1.06	26.4	Acc.

copyright is published under Lisensi Creative Commons Atribusi 4.0 Internasional.

As presented in Table 7, the effect of FSM caused by fluid motion within the oil tank increases the KG value or, equivalently, reduces the GM value. At an oil tank filling level of 30%, the FS correction, representing the increase in KG due to FSM, is 0.28 m for Barge 1, 0.29 m for Barge 2, and 0.28 m for Barge 3. However, the FS correction gradually decreases as the oil tank filling level increases. At a 50% filling level, the FS correction decreases to 0.22 m for Barge 1, 0.23 m for Barge 2, and 0.22 m for Barge 3.

From the various stability scenarios evaluated, Barge 1 consistently demonstrated the best stability performance compared with Barge 2 and Barge 3. This superior performance is attributed to its more favorable hull configuration, which provides larger righting arms throughout the range of heel angles. The higher GZ values indicate a greater restoring lever resulting from the relative movement between the center of buoyancy and center of gravity as the platform heels. In addition, the lower KG and higher GM_0 provide greater initial resistance to heeling. The hull geometry of Barge 1 also enables more effective redistribution of buoyancy during inclination, resulting in a larger GZ area and higher GZmax. Therefore, its superior stability results from the combined effects of hull geometry, buoyancy distribution, waterplane characteristics, and vertical weight distribution.

Despite its favorable stability performance, this study is limited to stability analyses under full-load and lightship conditions, including ballast management and the effects of wind turbines installed on the floating platform deck. However, seakeeping analysis considering environmental loads, particularly wind and wave actions, was not included. This aspect is important because the design of ships and floating platforms must also account for the intended operating sea conditions, as their safe operation is generally associated with specific environmental and wave conditions [22]–[25].

4. CONCLUSION

This study demonstrates that all three barge-type floating platform designs satisfy the requirements of the IMO Intact Stability Code under full-load conditions, confirming their suitability for supporting a renewable energy-powered oil skimmer system. Among the three configurations, Barge 1 consistently exhibited the best stability performance, as indicated by the highest GM, GZ, and GZ area, making it the most favorable design alternative. However, under lightship conditions, none of the platforms satisfied the minimum GZ_{max} angle criterion because of their relatively high KG values. The analysis further showed that a minimum ballast level of 75% is required to satisfy the intact stability criteria during the initial operating condition, whereas the ballast can be safely discharged once the oil tank reaches a minimum filling level of 45%. These findings highlight the importance of proper ballast management in maintaining adequate stability under varying loading conditions and provide a valuable reference for the design and operation of autonomous floating platforms for renewable energy-powered marine oil spill response systems. Future work will focus on analyzing the seakeeping performance of the floating platform under environmental loads, particularly wind and wave actions. In addition, the optimal placement of the wind turbines on the platform deck will be investigated to optimize energy generation while minimizing the effects of the additional loads on platform stability and seakeeping performance.

ACKNOWLEDGMENTS

The authors would like to express their sincere gratitude to the leadership of Bacharuddin Jusuf Habibie Institute of Technology (ITH) for providing financial support for this research. The authors also gratefully acknowledge all individuals and institutions who provided valuable technical assistance, constructive discussions, and other contributions throughout this study.

REFERENCES

[1] N. A. Annisa, P. Vionica, and U. Kamal, “Environmental Impact Analysis of Coastal Areas Due to Oil Spill in Karawang,” *Media Huk. Indones.*, vol. 2, no. 2, pp. 192–196, 2024, doi: https://doi.org/10.5281/zenodo.11261952.

[2] H. Grace, A. Belle, G. Margareth, T. Adefinola, and N. Febrayen, “Tanker Ship Accidents: Risks of Oil/Chemical (Hazardous Materials) Spills Affecting the Marine Environment, Response Challenges, and

copyright is published under Lisensi Creative Commons Atribusi 4.0 Internasional.

Tanker Safety Design Regulations," vol. 2, no. 1, pp. 326–346, 2025.
[3] C. S. De Claresya, R. H. T. Koestoer, W. S. Pranowo, and A. Cahyadi, "Pemodelan Pergerakan Tumpahan Minyak Sebagai Upaya Mitigasi Dampak Lingkungan di Perairan Lampung Timur, Indonesia," *J. Kelaut. Nas.*, vol. 18, no. 1, pp. 33–42, 2023, doi: http://dx.doi.org/10.15578/jkn.v18i1.12382.
[4] Supriyono, M. Yusuf, and D. T. Nurrohman, "Kajian Penanganan Tumpahan Minyak Menggunakan Oil Skimmer Tipe Rotary Disc pada Jenis Bahan Bakar Berbeda," *J. ECOTIPE*, vol. 8, no. 1, pp. 53–58, 2021, doi: https://doi.org/10.33019/jurnalecotipe.v8i1.1466.
[5] S. W. Ko, J. Y. Moon, S. M. Bae, C. S. Kim, and C. H. Park, "A Sponge-Type oil skimmer for highly efficient removal of floating Oils: Superabsorbent and oleophilic sponge with Nano-Scale interface roughness," *Appl. Surf. Sci.*, vol. 606, p. 154750, 2022, doi: https://doi.org/10.1016/j.apsusc.2022.154750.
[6] B. Herren, M. C. Saha, M. C. Altan, and Y. Liu, "Funnel-Shaped Floating Vessel Oil Skimmer with Joule Heating Sorption Functionality," *Polymers (Basel).*, vol. 14, no. 11, 2022.
[7] R. Manivel and R. Sivakumar, "Materials Today : Proceedings Boat type oil recovery skimmer," in *Materials Today: Proceedings*, Elsevier Ltd., 2020, pp. 470–473. doi: 10.1016/j.matpr.2019.06.632.
[8] D. Motorin, H. Roozbahani, and H. Handroos, "Development of a novel method for estimating and planning automatic skimmer operation in response to offshore oil spills," *J. Environ. Manage.*, vol. 318, p. 115451, 2022, doi: 10.1016/j.jenvman.2022.115451.
[9] Y. Kim, H. Kim, and D. Cho, "Evolutionary Approach to Optimal Oil Skimmer Assignment for Oil Spill Response : A Case Study," *Biomimetics*, vol. 9, no. 330, pp. 1–17, 2024.
[10] A. Yasim, M. Irsan, M. Dwiprayuda, M. Ikhsan, and M. Zulkifli, "A Comprehensive Study of Renewable-Powered Floating Oil Skimmer Design for Indonesian Oil Spill Recovery," *Kapal J. Ilmu Pengetah. dan Teknol. Kelaut.*, vol. 23, no. 1, pp. 37–48, Apr. 2026, doi: 10.14710/kapal.v23i1.79027.
[11] T. N. C. Bangun, A. Muntaha, and Sunardi, "STABILITAS KAPAL IKAN KATAMARAN SEBAGAI PENGGANTI KAPAL PURSE Oleh : Alumni Program Sarjana Departemen PSP FPIK Universitas Brawijaya," *ALBACORE*, vol. I, no. 1, pp. 13–21, 2017, doi: https://doi.org/10.29244/core.1.1.11-19.
[12] Mujiburrahman, H. Irawan, and M. Suprapto, "Uji Stabilitas Performa Perahu Fortable Jenis Katamaran Berbasis Plywood dan Fiberglass," *J. CRANKSHAFT*, vol. 8, no. 4, pp. 71–83, 2025, doi: https://doi.org/10.24176/cra.v8i4.16021.
[13] J. A. Hind, *Stability and Trim of Fishing Vessels and Other Small Ships*, 2nd ed. Wiley, 1982. [Online]. Available: https://books.google.co.id/books?id=bi4RAAAAYAAJ
[14] A. Yasim, R. Koekoeh Koentjoro Wibowo, D. Dwi Laksana, H. Indria Dwi Puspita, W. Sakinah, and P. Ganjar Widitiyo, "Hydrodynamics Comparison of V-shaped and U-shaped Hulls of 5 GT Fishing Vessels Based on the Characteristics of Southern Java Waters," 2022. [Online]. Available: www.ijerd.com
[15] L. L. Goldberg, *Principles of Naval Architecture, second revision*, vol. I. Jersey City-US: Society of Naval Architects and Marine Engineers, 1988.
[16] S. C. Misra, *Ships Marine Structures*. Florida, US: CRC Press, 2016. [Online]. Available: http://www.crcpress.com
[17] Nurhasanah and E. Yuliora, "The Analysis of Ship Stability of Ferry Ro-Ro Based on Loadcase Changes," *Wave J. Ilm. Teknol. Marit.*, vol. 20, no. 01, pp. 47–55, 2026, doi: https://doi.org/10.55981/wave.2026.14236.
[18] G. W. Kayadoe, H. V. Dien, and R. D. C. Pamikiran, "Kajian Tentang Stabilitas KM. Surya Prima Yang Dibuat Di Desa Borgo, Kec. Tanawangko, Kab. Minahasa," *J. Ilmu Dan Teknol. Perikan. Tangkap*, vol. 2, no. 1, pp. 19–22, 2015, doi: 10.35800/jitpt.2.1.2015.8330.
[19] IMO, *International Code of Intact Stability 2008*, 2020th ed. International Maritime Organization (IMO), 2020.
[20] H. I. D. Puspita, R. Rudianto, A. Yasim, and A. Nuruzzaman, "Analysis of Resistance and Stability In the Modification of Outrigged Fishing Boat Design in the Puger Water, JembeR," *J. Teknol. Perikan. dan Kelaut.*, vol. 16, no. 1, pp. 77–84, 2025, doi: https://doi.org/10.24319/jtpk.16.77-84.
[21] C. Huda, "Analisis Laju Korosi Material Aluminium 5083 Sebagai Aplikasi Bahan Lambung Kapal," *J. Pendidik. Tek. Mesin UNESA*, vol. 06, no. 02, pp. 17–24, 2017.
[22] A. Yasim, M. Soetardjo, and Mahrani, "Analisa Performa Seakeeping Kapal Ikan 5 GT Setelah Modifikasi Palkah dan Penggantian Mesin Utama (Studi Kasus KM. Nelayan 2017-572)," *J. Airaha*, vol. 14, no. 02, pp. 205–218, 2025, doi: https://doi.org/10.15578/ja.v14i2.780.
[23] A. Yasim, R. K. Koentjoro Wibowo, and K. Priohutomo, "Kajian Sinkronisasi Mesin Utama dan Propeller pada Kapal Perikanan Pasca Reparasi (Studi Kasus KM. Nelayan 2017-572)," *Wave J. Ilm. Teknol. Marit.*,

copyright is published under Lisensi Creative Commons Atribusi 4.0 Internasional.

vol. 15, no. 1, pp. 11–20, Aug. 2021, doi: 10.29122/jurnalwave.v15i1.4724.
[24] R. F. Kusnadi, P. G. Widityo, A. Yasim, and B. Ali, "Analysis of the Effect of Bilge Keel on the Rolling Motion of Ro-Ro Ferry Ship Using the Strip-Theory Method," *ROTOR*, vol. 16, no. 1, pp. 15–20, 2023.
[25] H. I. D. Puspita, A. Yasim, Rudianto, R. K. K. Wibowo, R. F. Kusnadi, and M. A. N. Akmal, "Pengaruh Penambahan Skeg Terhadap Olah Gerak dan Hambatan Kapal Nelayan di Pelabuhan Perikanan Puger, Jember," *J. Teknol. Perikan. dan Kelaut.*, vol. 14, no. 2, pp. 169–179, 2023, doi: https://doi.org/10.24319/jtpk.14.169-179.

copyright is published under Lisensi Creative Commons Atribusi 4.0 Internasional.